Supporting Information

Discovery, biosynthesis and antifungal mechanism of the polyene-polyol meijiemycin

Zhen Jie Low,‡[a] Juan Xiong,‡[a,c] Ying Xie,‡[a] Guang-Lei Ma,‡[a] Howard Saw,[a] Hoa Thi Tran,[a] Wong Soo Lin,[a] Li Mei Pang,[a] July Fong,[b] Peng Lu,[a] Jin-Feng Hu,[c] Liang Yang,[d] Yansong Miao*[a] and Zhao-Xun Liang*[a]

[a]*School of Biological Sciences, Nanyang Technological University, Singapore 637551.*
[b]*The Singapore Centre for Environmental Life Sciences Engineering (SCELSE), Nanyang Technological University, Singapore 637551.*
[c]*School of Pharmacy, Fudan University, Shanghai, China.*
[d]*School of Medicine, Southern University of Science and Technology, Shenzhen, Guangdong, China.*

Contents

Experimental Procedures

Isolation of *Streptomyces* sp. SD50 from mangrove sediment. *Streptomyces* sp. SD50 was isolated from a mangrove sediment sample and the pure colony isolate was spread onto MS agar (20 g/L soy flour, 20 g/L mannitol, 20 g/L Bacto agar) and cultured at 30ºC for 2-3 weeks until sporulation. Spores were harvested by gentle scrapping of aerial mycelia from plates flooded with sterile water using 1 mL pipette tip, followed by centrifugation at 8000 g for 5 min. Pelleted spores were re-suspended in 20% glycerol solution, aliquoted and kept frozen at 80 ºC for storage.

Genomic DNA isolation. The genomic DNA of *Streptomyces* sp. SD50 was extracted using a modified DNA salting out procedure for isolation of genomic DNA from Gram-positive bacteria.[1] *Streptomyces* sp. SD50 was cultured in liquid CRM culture for 2-4 days until it reached the late log phase of growth. Mycelium pellets were harvested by centrifuging the culture at 6,000 *g* for 15 min and re-suspended in 5 mL of SET buffer (75 mM NaCl, 25 mM EDTA pH 8.0, 20 mM Tris-HCl pH 7.5). The mycelium suspension was homogenized using a 15 mL handheld Dounce tissue grinder until finely dispersed. Lysozyme was added to the solution until a final concentration of 1 mg/mL and the mixture was incubated at 37ºC for 1-2 hr. The eventual protoplasts were lysed by adding 600 uL of 10% SDS solution. Another 140 uL of proteinase K (20 mg/mL in water) was added to the lysis mixture with gentle mixing, followed by a two-hour incubation at 55 ºC. Upon completion of protein digestion, 2 mL of 5 M NaCl solution was added to the mixture with gentle mixing. Upon cooling to 37 ºC, an equal volume of chloroform was added to the lysed cell solution and mixed by repeated gentle inversion for 5 min at ambient temperature. The emulsion was centrifuged at 4,500 g for 15 min and the aqueous layer was collected. The chloroform step was repeated until a clear aqueous layer was obtained. The aqueous phase was supplemented with RNase A to a final concentration 100 µg/mL and incubated at 37ºC for 1-2 hr for RNA digestion. High molecular weight genomic DNA was finally spooled from the aqueous mixture by adding 0.6 volume of isopropanol. The spooled DNA was washed twice with 5 mL of 70% aqueous ethanol and air dried under ambient conditions. Genomic DNA was subsequently re-dissolved in 10 mM Tris buffer, pH 8.0 and aliquoted into small volumes for storage in -20 ºC freezer.

Whole genome sequencing. Initial genome sequencing was performed using Illumina Miseq sequencing technology. A total of 214 contigs with an average size of 53,914 bp was obtained after *De novo* assembly of trimmed sequencing reads was performed using CLC Genomics Workbench (CLC bio, Denmark). Analysis of draft contigs revealed many truncated PKS genes in the genome, which complicated the genome mining efforts due to the difficulty of ascertaining relationship between those truncated genes. Hence, another round of genome sequencing was attempted with PacBio to obtain longer DNA contigs. The Single Molecule Real Time (SMRT) sequencing technology (Pacific Biosciences, California, USA) offered by PacBio RS II platform technology was used for obtaining long sequencing reads. A single SMRT cell was used and the sequencing run was performed 3 times. The long sequencing reads generated a 37 X coverage of the genome. A read quality value of 84 was achieved with 102,653 zero-mode-waveguides (ZMWs). Mean polymerase read length was 12,011 bp with mean reads of inserts (ROI) read length value of 10,013 bp. The PacBio reads were assembled into two contigs by Canu v1.6 and a final single contig of length 11,607,137 bases was obtained after the assembly validated by PCR amplification of the gap region.[2] The Illumina reads were mapped to the a single contig by CLC Genomics Workbench v10.0, and the .bam files for the mapped reads were extracted and used to polish the assembled contigs by Pilon v1.22[3] to further reduce sequencing errors.

Disruption of nanchangmycin and oxazolomycin BGCs using CRISPR/Cas9 method. All cloning steps were carried out using *E. coli* TOP10 (Invitrogen, US). Experimental procedures for construction of plasmids for CRISPR/Cas9 mediated gene mutation, conjugal transfer of plasmid from the donor *E coli* to *Streptomyces* sp. SD50, identification of true exconjugants, induction of *cas9* gene expression and plasmid curing are described previously by us.[4] To abolish the production of nanchangmycin, a Δ*nanA1* knockout mutant was generated by a 751 bp frameshift deletion of *nanA1* gene in the genome of *Streptomyces* sp. SD50. Likewise, oxazolomycin production was abolished by generating a 692 bp frameshift deletion of *ozmH* gene. The double Δ*nanA1*Δ*ozmH* knockout mutant of *Streptomyces* sp. SD50 was achieved by performing a subsequent *ozmH* gene deletion on a *Streptomyces* sp. SD50 Δ*nan* mutant. To screen for successful mutants, individual clones were cultured in liquid GYM at 30 ºC for 3 days for genomic DNA isolation.[5] Briefly, mycelia were harvested and re-suspended in 0.5 mL Lysis buffer (20 g CTAB, 100 mL Tris-HCl pH 8.0, 40 mL 0.5 M EDTA pH 8.0, 280 mL 5 M NaCl, 10 g PVP, top up to 1 L with ultrapure water and final pH of 5.0). The mixture was homogenized using a micro-pestle and incubated at 55 ºC for 15 min for lysis. An equal volume of chloroform was added to the mixture and vortexed vigorously for 1 min to ensure even mixing. The resultant emulsion was centrifuged at 10,000 g for 5 min. The aqueous layer containing genomic DNA was collected and mixed with equal volume of isopropanol. The mixture was centrifuged at 10,000 g for 5 min to pellet crude DNA precipitates. DNA was washed twice with 70% aqueous ethanol. The resultant pellets were dried at 55 ºC for 5 min and re-dissolved in sterile water for downstream analysis. Diagnostic PCR was performed to establish deletion of 751 bp and 692 bp in *nanA1* and *ozmH*, respectively.

Deletion of *mjmB* and *mjmE* genes using CRISPR/Cas9 method. The experimental procedures for CRISPR/Cas9-mediated genetic manipulation are as described above and elsewhere.[4] The *mjmB* gene was deleted by introducing a 926 bp frameshift deletion to *Streptomyces sp.* SD50 Δ*nanA1*Δ*ozmH* double mutant, resulting in the creation of a *Streptomyces sp.* SD50 Δ*nanA1*Δ*ozmH*Δ*mjmB* triple mutant. Similarly, a frameshift deletion of 772 bp was used to delete *mjmE*, which generated a *Streptomyces sp.* SD50 Δ*nanA1*Δ*ozmH*Δ*mjmE* triple mutant. Diagnostic PCR was performed to confirm the deletion of 926 bp and 772 bp in *mjmB* and *mjmE*, respectively.

Small-scale fermentation and metabolite profiling. To optimize the production of meijiemycin, *Streptomyces* sp. SD50 Δ*nanA1*Δ*ozmH* double mutant was cultured in various media conditions such as GYM agar, MS agar, liquid GYM, liquid Gly-YM (4 g/L glycerol 4 g/L yeast extract, 10 g/L malt extract), liquid mannitol-supplemented YM (20 g/L mannitol, 4 g/L yeast extract, 10 g/L malt extract) for 7 days at 30ºC. Extraction of compounds from both liquid and solid cultures was performed for metabolite profiling. Briefly, for solid medium extraction, the mutant strain incubated on a plate of agar for 10 days at 30 ºC was transferred into a beaker. 80 mL of acetone was added to the agar and the mixture was ground using a hand-held blender. Then, the mixture was centrifuge at 6,000 g for 15 min. The supernatant

was dried using the rotary evaporator for HPLC analysis. For liquid cultures, 30 mL of the cultures were centrifuge to separate the biomass and the culture media. The compounds from the biomass and liquid media were extracted using 30 ml of acetone and 25 ml ethyl acetate, respectively, by vigorous shaking. Both mixtures were centrifuged to at 6,000 g for 15 min. The acetone and ethyl acetate were collected and transferred into a glass flask to dry the compounds using the rotary evaporator. HPLC analysis of crude extracts was performed with Agilent Zorbax Eclipse XDB-C18 (4.6 mm x 250 mm, 5 μm) using an Agilent 1200 HPLC system equipped with DAD detector. A gradient elution with a binary solvent system at 1 mL/min was employed using water as mobile phase A and acetonitrile as mobile phase B. Both mobile phases were supplemented with 0.1% formic acid. LC program was set at 0-5 min 10% B-20% B, 5-35 min 20% B-70% B, 35-50 min 70% B-90% B, 50-60 min 90% B-100% B. The metabolites were monitored at λ = 220 nm, 264 nm, 280 nm, 360 nm and 420 nm.

Large-scale fermentation and isolation of meijiemycin. *Streptomyces* sp. SD50 was cultured in mannitol-supplemented YM (20 g/L mannitol, 4 g/L yeast extract, 10 g/L malt extract) liquid medium (5 X 800 mL in 2 L baffled Erlenmeyer flask) for 7 days at 30 ºC, 220 RPM. Mycelia was harvested by centrifugation and extracted by stirring with 4 L of methanol for 1 hr at ambient temperature. The organic extract was filtered using a Buchner funnel and dried using a rotary evaporator to afford a crude extract (~3 g). The crude extract was re-dissolved in 500 mL of methanol and extracted thrice with equal volumes of hexane to remove fatty material. The extract was dried completely and washed with 100 mL of ultrapure water to get rid of salts and other water miscible materials. The residual crude was soaked in minimal amount of dimethylformamide (DMF) and sonicated in a water bath to promote compound solubility. Methanol and ultrapure water were subsequently added to the crude solution at a final concentration of 1% (v/v) DMF, 60% methanol, 39% water. Meijiemycin was purified from the crude using Shimadzu Prominence Preparative HPLC system equipped with an ACE C18 semi-prep column (10 mm X 250 mm, 5 μm). A gradient elution program was set up with the following conditions: 0-40 min 75%-90% aqueous methanol, 40-50 min 100% aqueous methanol. A flow rate of 4 mL/min was employed for the reversed phase column chromatography procedure. Fractions containing pure meijiemycin, which eluted at t = 36 min, were pooled and dried using a rotary evaporator. A total of 25 mg of meijiemycin was isolated as a dark yellow solid.

Structural determination. The ^{13}C NMR spectrum exhibited 66 carbon signals, which were attributed to two carbonyls, seven methyls, thirteen methylenes, forty-two methines, and two quaternary carbons according to HSQC experiments. Further interpretation of the two-dimensional NMR (COSY, HSQC, HMBC, and NOESY) data revealed the presence of five aliphatic and two vinyl methyl groups, eleven oxymethine groups, eleven double bonds (including a hexaene and a triene), an aminosugar moiety, and two carboxyl groups (Figs. S13–20). The four separate spin systems suggested by COSY correlations were connected through HMBC correlations (Fig. S3) to establish the connectivity of the carbon skeleton. The proton H-38 shows large vicinal-coupling constants ($J_{\text{H-37, 48}} = J_{\text{H-38, 39}} = 10.5$ Hz) and is most likely in a six-membered ring, supporting that C-35 is connected to C-39 to form an intramolecular hemiketal group. The *trans*-hexaene conjugated system (C-42~C-54) was readily identified based on its characteristic UV absorptions at λ_{max} 340 (4.71), 356 (4.90), and 378 (4.90) nm (Fig. S21).[6-8] This deduction was further confirmed by COSY and HMBC correlations (Figure S3).

For the geometry of the olefines in this moiety, the large coupling constants observed between H-42 and H-43 (J = 15.0 Hz), and between H-52 and H-53 (J = 15.0 Hz) established the 42*E*, 52*E*-configuraiton. Overlapping of the signals from H-44 to H-51 hampered the observation of any ^3J coupling constant or NOE correlation that could have directly assessed the *Z* or *E* configuration of these double bonds. However, analysis of the aforementioned UV spectroscopic data suggested that the double bonds in the chromophore are all in the *trans* (i.e., *E*) configuration.[6-8] Consistent with this, the ^{13}C NMR data assigned to this hexaene moiety, which appeared in a relatively narrow range (δ 130.7 ~ 134.6, Table S3), were found to be comparable with those in the reported all-*trans* hexaene-containing compounds.[9,10] The geometrical configurations of the rest olefinic bonds (i.e., $\Delta^{2, 6, 8, 10, 26}$) were assigned based on the vicinal coupling constants and NOE correlations (Fig. S4). The remaining unassigned stereochemistry of the hydroxy groups and aliphatic methyl groups were assigned based on the stereo-selectivity of the ketoreductase (KR) domains of the *mjm* PKSs as we will discuss later. Similar approaches have been adopted for configurational assignment of highly complex natural products such as lobosamide and salinilactam.[11,12] While the NOE correlations between H_3-55 and H-7 supported the presence of a *cis*-olefin generated by module 24, the coupling constant (11.2 Hz) between H-8 and H-9 and the NOE correlation between H-9 and H-10 also supported a *cis*-olefin generated by module 23. As for the relative configuration of the hemiketal ring (C-35~C-39), the large vicinal coupling constants observed for H-38 (J = 10.5, 10.5 Hz) implied a chair conformation (Fig. S5) for this ring with H-37, H-38, and H-39 being in axial positions. Moreover, the NOE correlations of H-36a with H_2-34 and H-38 (Figs. S4 and S5) supported an equatorial α-position for CH_2-34 and the positioning of OH-35 on the β-face of the hemiketal ring.[13-15]

The NMR data suggested that meijiemycin contains a perosamine sugar moiety, which was evident from the sequential COSY correlations from H-1′ to H_3-6′ and the HMBC correlations of H_3-6′ with C-4′ and C-5′ (Fig. S3). This is a contrast to the more common mycosamine sugar found in many macrocyclic polyene-polyols such as natamycin, amphotericin B, and nystatin.[16-18] The NOE correlations arisen from the 1, 3-diaxial interaction between H-1′ and both H-3′ and H-5′ are indicative of the β-type glycosidic linkage, as well as the α-orientations of 3′-OH and 6′-Me. The H-2′ was concluded to be equatorially β-oriented based on a weak coupling (near 0 Hz) observed between H-1′ and H-2′. Besides, H-4′ adopts an axial α-orientation as evidenced by the large vicinal-coupling constants (J = 10.2 Hz) with both H-3′ and H-5′. Consistent with this, H-4′ did not show any NOE correlations with any other protons (Fig. S4). Moreover, the NOE correlations of H-1′ with H-40β/H-43, of H-41 with H-43, and of H-38 with H-40α indicated the sugar to be located at the β-orientation of *trans*-hexaene chromophore plane (Fig. S5).[13-15]

Both C-12/C-13 and C-19/C-20 were assigned as *anti*-form based on their large coupling constants ($^3J_{\text{H-12,H-13}} = 9.0$ Hz, $^3J_{\text{H-19,H-20}} = 9.2$ Hz) and key NOE correlations (Fig. S5).[19] The relative configurations of C-15/C-16/C-17/C-18 were deduced as *anti/anti/syn* by comparison of the ^{13}C chemical shifts of the methine C-16 and methyl C-58 with those summarized in database (Fig. S6). Similarily, The relative configurations of C-29/C-31/C-33 were elucidated as *syn/syn* by application of Kishi's universal NMR database (Fig. S6).[20,21]

Attempts to determine the absolute configuration based on chemical degradation (periodate oxidation and derivatization) were not sucessful due to the chemical liability of meijiemycin and complexity of the degradation products. Therefore, we focused on the bioinformatics analysis of *mjm* gene cluster (Table S2, Figs. S8-S10). The proposed absolute configurations predicted by the KR domains were summarized in Table S5, which in turn confirmed the validity of the relative configurational assignments by NMR spectroscopy. Therefore, based on genetic analysis and the NMR data analyses, we proposed the absolute configuration of meijiemycin (**1**) as 2*E*,5*R*,6*Z*,8*Z*,10*E*,12*S*,13*R*,15*R*,16*R*,17*R*,18*R*,19*R*,20*R*,26*E*,29*S*,31*S*,33*S*,35*R*,37*S*,38*R*,39*S*,41*R*,42*E*,44*E*,46*E*,48*E*,50*E*,52*E*.

Meijiemycin (**1**). UV (MeOH) λ_{max} (log ε) 277 (4.48), 324 (4.38), 340 (4.71), 356 (4.90), 378 (4.90) nm; ^{1}H NMR (400 MHz, in C_5D_5N) δ 7.51 (1H, ddd, J = 15.6, 7.0, 6.7 Hz, H-3), 6.91 (1H, dd, J = 15.4, 11.6 Hz, H-10), 6.74 (1H, dd, J = 15.0, 10.7 Hz, H-43), 6.62 (1H, br d, J = 11.0 Hz, H-7), 6.43 (1H, dd, J = 11.0, 11.0 Hz, H-8), 6.36 (1H, d, J = 15.6 Hz, H-2), 6.25 (dd, m, H-44), 6.21-6.40 (7H, m, H-45 to H-50), 6.14 (1H, m, H-52), 6.12 (1H, dd, J = 15.4, 7.0 Hz, H-11), 6.10 (1H, dt, J = 15.0, 6.3 Hz, H-42), 6.08 (1H, dd, J = 11.6, 11.0 Hz, H-9), 5.71 (1H, dt, J = 15.0, 7.5 Hz, H-27), 5.69 (1H, m, H-53), 5.58 (1H, dt, J = 15.0, 7.5 Hz, H-26), 5.23 (1H, m, H-37), 5.23 (1H, dd, J = 7.5, 4.5 Hz, H-5), 5.16 (1H, m, H-33), 5.13 (1H, m, H-41), 4.95 (1H, br s, H-1′), 4.93 (1H, m, H-39), 4.75 (1H, m, H-15), 4.52 (1H, m, H-31), 4.41 (1H, m, H-13), 4.39 (1H, br s, H-2′), 4.21 (1H, m, H-29), 3.94 (1H, br d, J = 9.2 Hz, H-19), 3.87 (1H, br d, J = 7.9 Hz, H-17), 3.81 (1H, m, H-3′), 3.59 (1H, m, H-5′), 3.30 (1H, dd, J = 10.2, 10.2 Hz, H-4′), 2.98 (1H, dd, J = 10.5, 10.5 Hz, H-38), 2.82 (1H, ddd, J = 15.8, 7.5, 7.0 Hz, H-4a), 2.73 (1H, m, H-36a), 2.65 (1H, m, H-12), 2.56 (1H, ddd, J = 15.8, 6.7, 4.5 Hz, H-4b), 2.46 (1H, m, H-40a), 2.45 (1H, m, H-28a), 2.41 (1H, m, H-28b), 2.40 (1H, m, H-16), 2.39 (1H, m, H-40b), 2.17 (1H, dd, J = 11.0, 4.9 Hz, H-34a), 2.07 (1H, m, H-18), 2.07 (1H, m, H-14a), 2.07 (1H, m, H-34b), 2.06 (1H, m, H-21a), 2.05 (3H, br s, H_3-55), 2.02 (2H, m, H_2-25), 1.96 (1H, m, H-36b), 1.96 (2H, m, H_2-30), 1.90 (2H, m, H_2-32), 1.87 (1H, m, H-14b), 1.76 (1H, m, H-20), 1.65 (1H, d, J = 7.0 Hz, H-54), 1.46 (1H, d, J = 5.4 Hz, H-6’), 1.36 (2H, m, H_2-24), 1.36 (2H, m, H_2-23), 1.27 (3H, d, J = 6.7 Hz, H_3-56), 1.26 (3H, d, J = 6.7 Hz, H_3-58) 1.25 (1H, m, H-21b), 1.22-1.35 (2H, m, H_2-22), 0.98 (3H, d, J = 6.6 Hz, H_3-57), 0.85 (3H, d, J = 6.3 Hz, H_3-59); ^{13}C NMR (400 MHz, in DMSO-d_6) δ 174.7 (C-60), 168.0 (C-1), 145.2 (C-3), 141.3 (C-6), 139.2 (C-11), 134.2 (C-42), 133.9 (C-51), 133.1 (C-43), 132.4 (C-26), 131.5 (C-52), 131.1-133.9 (C-44 to C-50), 130.7 (C-53), 129.1 (C-9), 127.3 (C-27), 125.3 (C-10), 124.7 (C-2), 122.3 (C-8), 121.6 (C-7), 98.9 (C-1′), 97.6 (C-35), 78.8 (C-17), 76.1 (C-41), 74.1 (C-19), 73.3 (C-3′), 72.2 (C-5′), 70.8 (C-13), 70.6 (C-2′), 69.4 (C-29), 68.9 (C-15), 67.6 (C-31), 67.4 (C-5), 66.5 (C-39), 66.3 (C-33), 65.9 (C-37), 58.1 (C-38), 54.7 (C-4′), 46.6 (C-34), 45.8 (C-32), 44.6 (C-30), 44.5 (C-36), 43.7 (C-12), 42.2 (C-16), 41.3 (C-28), 38.9 (C-40), 38.5 (C-4), 37.1 (C-14), 36.3 (C-20), 34.5 (C-18), 32.9 (C-21), 32.7 (C-25), 29.8 (C-24), 29.8 (C-23), 26.5 (C-22), 18.8 (C-55), 18.7 (C-54), 18.6 (C-6’), 17.2 (C-56), 15.8 (C-59), 12.1 (C-57), 11.4 (C-58). HRMS *m/z* 1216.7357 $[M+H]^+$ (calculated for $C_{66}H_{105}NO_{19}H^+$, 1216.7359).

Antifungal activity assay. The minimal inhibitory concentration (MIC) was determined via a modified broth microdilution assay protocol adopted for aerobic bacteria.[22] Lyophilized meijiemycin powder was initially dissolved in DMSO and diluted with sterile water to form 2% DMSO aliquots for assays. 50 uL of fungal culture, containing 1 million CFU in RPMI 1640 medium, was spiked with equal volume of compound solution and incubated at 30 °C with 180 RPM for 40 hr. Antifungal susceptibility was measured using a range of compound concentration that from 0.25 ug/mL to 128 ug/mL via serial two-fold dilution. MIC values were determined from the growth data obtained via turbidometry.[23]

Cytotoxicity assay. Cytotoxic effects in RAW264.7 macrophage cells were assessed by culturing macrophages (5×10^5) with different concentrations of the antifungal compounds (0.1–128 μg/mL) in 96-well tissue culture plates at 37°C in 5% CO_2 for 48 h. Cell viability was determined by the colorimetric MTT assay [3-(4,5-dimethylthiazol-2-yl)-2,5-diphenyltetrazolium bromide]. The cytotoxicity results were displayed as percentage of cell viability comparing with untreated cells (100% of viability). Absorbance of the solubilized MTT formazan product was spectrophotometrically measured at 540 nm using a SpectraMax 190 microplate reader. All samples were run in triplicate and analyzed on the same day to minimize day-to-day variation. Experiments were performed in triplicates, and the results are shown as the mean ± SD.

Preparation of liposome-encapsulated and Alexa Fluor™ 488 labelled Meijiemycin. Meijiemycin was first conjugated with the Alexa Fluor™ 488 (ThermoFisher, Cat. No. A10235) dye following manufacture instructions. The dye-labeled meijiemycin was dissolved in methanol and mixed thoroughly with the lipid L-α-phosphatidylcholine (Egg-PC, chicken, Avanti Polar Lipids) in chloroform with a molar ratio of 99 to 1 before evaporating the organic solvent through lyophilization. Afterwards, 100 mM PBS pH 7.4 buffer was added to the dry film to form meijiemycin conjugated liposome followed by 30 min of sonication to reduce the size of liposome.

Treatment of *C. albicans* with meijiemycin during hyphae growth. The overnight culture of *C. albicans* cells at 30°C were diluted 100 times in YPD (10 g per liter yeast extract, 20 g per liter peptone, 20 g per liter glucose) medium, and the hyphae growth was induced by 37°C for 3 hours with meijiemycin or the control DMSO added. The hyphae length was measured from the center of the bud neck to the bud tip with the segmented line tool in Image J.

Monitoring ergosterol distribution using the fluorescence probe filipin. The *C. albicans* hyphae cells culture (9 ml) treated with or without meijiemycin were fixed by adding 37.5% formaldehyde to a final concentration of 4% in the culture for 10 min at 25 °C. And the cells were collected by centrifugation at 3,000 g for 2 min and washed by sterilized water twice before re-suspending in 1 ml of sterilized water. 200 μl of cells were then stained by 4 μl 5mg/ml filipin at dark for 15min before mounting to the cover slip and imaged by florescence microscope.

Liquid yeast cell growth assay. The overnight saturated budding yeast culture was re-inoculated in fresh YPD medium from O.D.600=0.2 and culture around 3 hours until O.D.600 reached 0.8 in 30 °C. Then the cell culture was diluted to O.D.600=0.1 with meijiemycin added at the desired concentrations, 130 μl of cell culture was applied in each well of 96 well transparent bottom microplate sealed with a Breathe-Easy® sealing film (Diversified Biotech). Each tested condition contained four replicates that were growing at 30 °C for 16 hours. The O.D.600 of each well was measured and recorded by the Cytation™ 5 plate reader machine (BioTek® Instruments, Inc.) every 15min, and the microplate was kept shaking between each measurement to avoid cells precipitation. The collected data were subjected to GraphPad Prism 6 (GraphPad, San Diego, CA, USA) to generate a growth curve with an averaged O.D.600 and error bars in SD.

Live-cell fluorescence imaging. The budding yeast cell expressing the fluorescence markers were cultured in synthetic complete (6.7 g per liter of yeast nitrogen base, 20 g per liter of glucose with essential amino acid) medium without tryptophan (to minimize auto-fluorescence)

for overnight, and re-inoculated to fresh synthetic complete medium starting from O.D.600=0.2 and cultured until around 0.6. Afterwards, the cells were immobilized to Concanavalin A (1 mg/ml)-coated coverslips and imaged by wild field microscope Leica DMi8 (Leica Microsystems, equipped with ORCA-Flash4.0 LT scientific CMOS camera (Hamamatsu Photonics, Japan) and Leica 100x oil immersion objective lens (NA 1.4). For the whole-cell imaging, images were acquired continuously at a 0.25 μm interval for a total range of 7.5 μm in the z-direction, using an exposure time of 200 ms and 1x binning. To quantify the lifetime of Abp1-RFP, images were acquired continuously at rates of 1s per frame and 90 frames in total. Whereas for Sla1-GFP, images were acquired continuously at rates of 1s per frame and 180 frames in total. The movies of Abp1-RFP and Sla1-GFP were then used to generate the kymograph from ImageJ, the trajectory of Abp1-RFP or Sla1-GFP with invagination tail were used to quantify the lifetime of an individual protein. Meijiemycin treated *C. albicans* were immobilized to Concanavalin A (1mg/ml)-coated coverslips and removed the remaining medium to reduce the background signal, then supplemented with fresh YPD medium before imaging.

SUPPORTING INFORMATION

Table S1. Primers used in this study.

Primer name	Sequence (5' -> 3')	Purpose
Nanchang ctg20-33 sgrna F	CATGCCATGGcgagccgccgctgaaccgcaGTTTTAGAGCTAGAAATAGC	sgRNA amplifcation for *nanA1* KO
sgRNA R	ACGCCTACGTAAAAAAAGCACCGACTCGGTGCC	
oxazolomycin ctg6-179 sgrna F	CATGCCATGGtcgctggcgctgcacaagagGTTTTAGAGCTAGAAATAGC	sgRNA amplifcation for *ozmH* KO
sgRNA R	ACGCCTACGTAAAAAAAGCACCGACTCGGTGCC	
MjmE sgrna F	CATGCCATGGTGGACCGCCATCGTGAGCACGTTTTAGAGCTAGAAATAGC	sgRNA amplifcation for *mjmE* KO
sgRNA R	ACGCCTACGTAAAAAAAGCACCGACTCGGTGCC	
MjmB sgrna F	CATGCCATGGcggggagcagatctgctcctGTTTTAGAGCTAGAAATAGC	sgRNA amplifcation for *mjmB* KO
sgRNA R	ACGCCTACGTAAAAAAAGCACCGACTCGGTGCC	
sgRNA check F	CACAGGAAACAGCTATGACC	sgRNA sequencing
sgRNA check R2	TCAGCCCAGATCCCCGATCC	
sgRNA check R	ACCCCCCATTCAAGAACAGC	
Nanchang left F40	TCGTCGAAGGCACTAGAAGGTGAACCTGATCCTGGCCGAG	Homologous recombination template construction for pCRISPR-Cas9-nanA1
Nanchang left R40	GTGACATTGGATACGACGGGAGGTGACCCAGCAGTTCGTC	
Nanchang right F20	CCCGTCGTATCCAATGTCAC	
Nanchang right R40	GGTCGATCCCCGCATATAGGGCTGATCCCGAAGAACTCCG	
oxazolo left F40	TCGTCGAAGGCACTAGAAGGGAACATCGGGTCGAAGGAGG	Homologous recombination template construction for pCRISPR-Cas9-ozmH
oxazolo left R40	GCTGCGCTATCTGTACGTGCAACAGCTTCCTCGCCCACTA	
oxazolo right F20	GCACGTACAGATAGCGCAGC	
oxazolo right R40	GGTCGATCCCCGCATATAGGCGGCGTGGTCTATCTCGAGA	
mjmE left F40	TCGTCGAAGGCACTAGAAGGTCCACGGTCGTACCCAGCTC	Homologous recombination template construction for pCRISPR-Cas9-mjmE
mjmE left R40	GGTGCGCTGTCGCTGGAAGAGAGTTCTGGTCCGCCGTCGAA	
mjmE right F20	TCTTCCAGCGACAGCGCACC	
mjmE right R40	GGTCGATCCCCGCATATAGGCAAGATGGTGATGGCGCTGC	
mjmB left F40	TCGTCGAAGGCACTAGAAGGTGAAGTCGAACCTCGGTCAC	Homologous recombination template construction for pCRISPR-Cas9-mjmB
mjmB left R40	CGGAGCTTGTCGGCGGTGCCCTGGACTCCCAGTTCGTTGT	
mjmB right F20	GGCACCGCCGACAAGCTCCG	
mjmB right R40	GGTCGATCCCCGCATATAGGGATCGAGCCGAGCCACATGG	
pcrispr-cas9 seq	TGAGGCTTGCAGGGAGTCAA	HDR template sequencing
pcrispr-cas9 seq R	CGTCGCTCTCTGGCAAAGCT	
Nan check F	GTACTGCCGGATCGGTCCAC	Validation of *nanA1* deletion
Nan check R	CATGCCGGTCAACGAGGCGT	
Oxa check F	GAGTCGATGCCGTAGTGCTC	Validation of *ozmH* deletion
Oxa check R	CGATGAACTCCTGCGGCT	
mjmE check F	GCGATTCCAGGTCTTCCTGT	Validation of *mjmE* deletion
mjmE check R	ATGTGCACACCATCCTGGAG	
mjmB check F	GTGTCCTCGTTCGGGATCAG	Validation of *mjmB* deletion
mjmB check R	GGCCTTCTCATGCCTGTTCT	

Table S2. Genes in the meijiemycin biosynthetic gene cluster and their putative functions.

Gene	Size (amino acid)	Closest homolog [source]	Identity/Similarity (%)	proposed function	UniProt ID
ctg1-17	335	NADPH:quinone reductase [*Streptomyces griseochromogenes*]	85/93	unknown	A0A1B1AY81
mjmR	224	LuxR family transcriptional regulator [*Streptomyces bingchenggensis* BCW-1]	97/98	Transcriptional regulator	D7C2C5
mjmSI	345	GDP-mannose 4,6-dehydratase [*Streptomyces bingchenggensis* BCW-1]	98/99	GDP-mannose 4,6-dehydratase	D7C2C4
mjmB	9637	Beta-ketoacyl synthase [*Streptomyces* sp. NBS 14/10]	95/96	Polyketide synthase	A0A229GXM4
mjmOII	63	Ferredoxin-1 [*Streptomyces* sp. NBS 14/10]	98/98	Electron transfer	A0A229GYB0
mjmOI	391	Cytochrome P450 [*Streptomyces bingchenggensis* BCW-1]	98/99	Carboxylase	D7C2C0

mjmSIII	467	MGT family glycosyltransferase [*Streptomyces* sp. NBS 14/10]	99/100	Glycosyltransferase	A0A229GX50
mjmU	35	Flavin oxidoreductase (*Pandoraea* sp. ISTKB)	57/61	unknown	A0A1E3LP46
mjmC	7495	Polyketide synthase (*Streptomyces* sp. NBS 14/10)	95/96	Polyketide synthase	A0A229GX27
mjmD	1748	Uncharacterized protein (*Streptomyces* sp. NBS 14/10)	96/97	Polyketide synthase	A0A229GXC1
mjmE	9157	Modular polyketide synthase [*Streptomyces bingchenggensis* BCW-1]	96/97	Polyketide synthase	D7BRE1
mjmF	3633	Modular polyketide synthase [*Streptomyces bingchenggensis* BCW-1]	93/95	Polyketide synthase	D7BRE0
mjmG	1371	RifB protein [*Streptomyces bingchenggensis* BCW-1]	95/97	Polyketide synthase	D7BRD9
mjmH	4034	Beta-ketoacyl synthase [*Streptomyces* sp. NBS 14/10]	77/84	Polyketide synthase	A0A229H3V340
mjmSII	351	Perosamine synthetase [*Streptomyces bingchenggensis* BCW-1]	97/98	Perosamine synthetase	D7BRD5
mjmA	9914	Short-chain dehydrogenase [*Streptomyces* sp. NBS 14/10]	94/96	Polyketide synthase	A0A229H394
ctg1-34	136	Glyoxalase [*Streptomyces* sp. NBS 14/10]	95/97	unknown	A0A229H307

Table S3. ^{1}H and ^{13}C NMR spectroscopic data of meijiemycin.

Position	δ_H (mult., *J* in Hz)		δ_C	
	in DMSO-d_6	in pyridine-d_5	in DMSO-d_6	
1			168.0	
2	5.77 (d, 15.1)	6.36 (d, 15.6)	124.7	
3	6.72 (ddd, 15.1, 7.0, 6.7)	7.51 (ddd, 15.6, 7.0, 6.7)	145.2	
4	Ha: 2.39 (m)	Ha: 2.82 (ddd, 15.8, 7.5, 7.0)	38.5	
	Hb: 2.24 (m)	Hb: 2.56 (ddd, 15.8, 6.7, 4.5)		
5	4.68 (dd, 6.9, 5.8)	5.23 (dd, 7.5, 4.5)	67.4	
6			141.3	
55	1.76 (br s)	2.05 (br s)	18.8	6-Me
7	6.30 (br d, overlapped)	6.62 (br d, 11.0)	121.6	
8	6.12 (dd, 11.2, 11.2)	6.43 (dd, 11.0, 11.0)	122.3	
9	5.88 (dd, 11.6, 11.2)	6.08 (dd, 11.6, 11.0)	129.1	
10	6.51 (dd, 15.1, 11.6)	6.91 (dd, 15.4, 11.6)	125.3	
11	5.73 (dd, 15.1, 6.3)	6.12 (dd, 15.4, 7.0)	139.2	
12	2.26 (m)	2.65 (m)	43.7	
56	0.98 (d, 6.7)	1.27 (d, 6.7)	17.2	12-Me
13	3.63 (m)	4.41 (brd, 9.0)	70.8	
14	Ha: 1.38 (m)	Ha: 2.07 (m)	37.1	
	Hb: 1.22 (m)	Hb: 1.87 (m)		
15	3.96 (m)	4.75 (m)	68.9	
16	1.78 (m)	2.40 (m)	42.2	
57	0.69 (d, 6.3)	0.98 (d, 6.6)	12.1	16-Me
17	3.31 (br d, 7.6)	3.87 (br d, 7.9)	78.8	
18	1.75 (m)	2.07 (m)	34.5	
58	0.87 (d, 6.7)	1.26 (d, 6.7)	11.4	18-Me
19	3.45 (br d, 9.2)	3.94 (br d, 9.2)	74.1	
20	1.38 (m)	1.76 (m)	36.3	
59	0.70 (d, 6.3)	0.85 (d, 6.3)	15.8	20-Me
21	Ha: 1.67 (m)	Ha: 2.06 (m)	32.9	
	Hb: 0.98 (m)	Hb: 1.25 (m)		
22	Ha: 1.34 (m)	1.22~1.35	26.5	
	Hb: 1.16 (m)	1.22~1.35		
23	1.33 (2H, m)	1.36 (2H, m)	29.8	
24	1.33 (2H, m)	1.36 (2H, m)	29.8	
25	1.96 (2H, overlapped)	2.02 (2H, overlappled)	32.7	
26	5.41 (m)	5.58 (dt, 15.0, 7.5)	132.4	
27	5.41 (m)	5.71 (dt, 15.0, 7.5)	127.3	
28	Ha: 2.09 (m)	Ha: 2.45 (m)	41.3	
	Hb: 2.03 (m)	Hb: 2.41 (m)		
29	3.62 (m)	4.21 (m)	69.4	
30	1.45 (2H, m)	1.96 (2H, m)	44.6	

31	3.77 (m)	4.52 (m)	67.6	
32	1.49 (2H, m)	1.90 (2H, m)	45.8	
33	4.20 (m)	5.16 (m)	66.3	
34	Ha: 1.67 (m) Hb: 1.58 (m)	Ha: 2.17 (dd, 11.0, 4.9) Hb: 2.07 (dd, overlapped)	46.6	
35			97.6	
36	Ha: 1.90 (m) Hb: 1.19 (m)	Ha: 2.73 (m) Hb: 1.96 (m)	44.5	
37	3.96 (m)	5.23 (m)	65.9	
38	1.95 (dd, overlapped)	2.98 (dd, 10.5, 10.5)	58.1	
60			174.7	38-COOH
39	3.81 (m)	4.93 (m)	66.5	
40	Ha: 1.86 (m) Hb: 1.52 (m)	Ha: 2.46 (m) Hb: 2.39 (m)	38.9	
41	4.32 (m)	5.13 (m)	76.1	
42	5.64 (m)	6.10 (dt, 15.0, 6.3)	134.6	
43	6.30 (dd, overlapped)	6.74 (dd, 15.0, 10.7)	133.1	
44	6.22~6.30	6.25 (dd, overlapped)	131.1~133.9	
45	6.22~6.30	6.21~6.40	131.1~133.9	
46	6.22~6.30	6.21~6.40	131.1~133.9	
47	6.22~6.30	6.21~6.40	131.1~133.9	
48	6.22~6.30	6.21~6.40	131.1~133.9	
49	6.22~6.30	6.21~6.40	131.1~133.9	
50	6.22~6.30	6.21~6.40	131.1~133.9	
51	6.31 (dd, overlapped)	6.21~6.40	133.9	
52	6.13 (dd, 15.1, 10.7)	6.14 (dd, overlapped)	131.5	
53	5.75 (m)	5.69 (m)	130.7	
54	1.75 (d, 7.0)	1.65 (d, 7.0)	18.7	
1'	4.36 (br s)	4.95 (br s)	98.9	
2'	3.63 (dd, overlapped)	4.39 (br s)	70.6	
3'	3.18 (dd, overlapped)	3.81 (dd, overlapped)	73.3	
4'	2.46 (dd, overlapped)	3.30 (dd, 10.2, 10.2)	54.7	
5'	3.05 (m)	3.59 (m)	72.2	
6'	1.13 (d, 6.0)	1.46 (d, 5.4)	18.6	

Table S4. Strains used in this study.

Strain name	Genotype	Note	Source
E. coli TOP10	F$^-$ *mcr*A Δ(*mrr-hsd*RMS-*mcr*BC) φ80*lac*ZΔM15 Δ*lac*X74 *rec*A1 *ara*D139 Δ(*ara-leu*)7697 *gal*U *gal*K λ$^-$ *rps*L(Str^R) *end*A1 *nup*G	*E. coli*	Invitrogen
Streptomyces sp. SD50	-	*Streptomyces*	This study
Δ*nanA1* mutant	Δ*nanA1*	*Streptomyces*	This study
Δ*ozmH* mutant	Δ*ozmH*	*Streptomyces*	This study
Δ*nanA1*/Δ*ozmH* double mutant	Δ*nanA1,* Δ*ozmH*	*Streptomyces*	This study
Δ*N*Δ*O*Δ*mjmB* triple mutant	Δ*nanA1,* Δ*ozmH,* Δ*mjmB*	*Streptomyces*	This study
Δ*N*Δ*O*Δ*mjmE* triple mutant	Δ*naA1,* Δ*ozmH,* Δ*mjmB*	*Streptomyces*	This study
Candida albicans DF2162R	-	*C. albicans clinical isolate*	NUHS

Aspergillus fumigatus CBS133.61	-	*Aspergillus*	ATCC
Aspergillus westerdijkiae CBS112803	-	*Aspergillus*	ATCC
YMY2045	*ura3/ura3 his1::hisG/his1::hisG arg4::hisG/arg4::hisG*	*C. albicans*	Wang *et.al.*[24]
YMY2046	MATa *his3-Δ200 leu2-3, 112, ura3-52* Lsp1-GFP::His3 Pil1-Cherry::KanMX	*S. cerevisiae*	This study
YMY2047	MATa *his3-Δ200 leu2-3, 112, ura3-52* Sla1-GFP::Hygo Abp1-RFP::His3	*S. cerevisiae*	This study
Murine RAW264.7 macrophage	-	*Mammalian*	ATCC

Table S5. Proposed absolute configurations of meijiemycin based on the bioinformatics analysis of the sequences and conserved residues of the KR domains and relative configuration determined by NMR spectroscopic method.

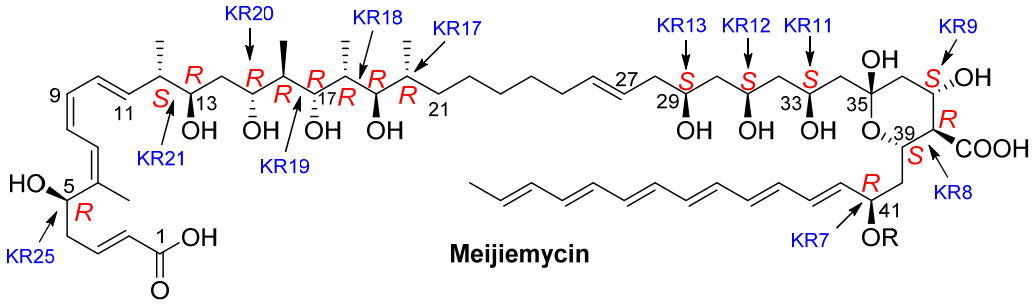

Domain	KR type	Predicted by the sequence analysis of KR domains		Assigned by NMR spectroscopic data [c]
		Keatinge-Clay "*RS*" system[a]	Classical *RS* system[b]	
mjmKR7	A1	"*S*" (C-41)	41*R*	*anti* (C41/39)
mjmKR8	A2	"*S,S*" (C-38,39)	38*R*,39S	*anti* (C38/39)
mjmKR9	B1	"*R*" (C-37)	37*S*	*anti* (C37/38)
mjmKR11	B1	"*R*" (C-33)	33*S*	*syn* (C33/31)
mjmKR12	B1	"*R*" (C-31)	31*S*	*syn* (C31/33)
mjmKR13	B1	"*R*" (C-29)	29*S*	*syn* (C29/31)
mjmKR17	B1	"*R*" (C-20)	20*R*	*anti* (C19/20)
mjmKR18	B1	"*R,R*" (C-18,19)	18*R*,19*R*	*anti* (C18/19)
mjmKR19	A2	"*S,S*" (C-16,17)	16*R*,17*R*	*anti* (C16/17)
mjmKR20	A2	"*S*" (C-15)	15*R*	*anti* (C15/16)
mjmKR21	B1	"*R,R*" (C-12,13)	12*S*,13*R*	*anti* (C12/13)
mjmKR25	A1	"*S*" (C-5)	5*R*	--

[a]The "*R*" and "*S*" configurations denote a deviation from the classical *RS* system: For the configuration assignment at the *β*-position of the extended polyketide chain, *γ*-carbon was regarded as the lowest priority after the hydrogen; when discussing the chirality at the *α*-position, the *α*-substituent is given as the lowest priority after the hydrogen. In both cases, the carboxyl end of the chain is given the highest priority. [b]The configuration was determined based on the Cahn-Ingold-Prelog system. [c]Relative configuration was assigned by NMR spectroscopic analysis.

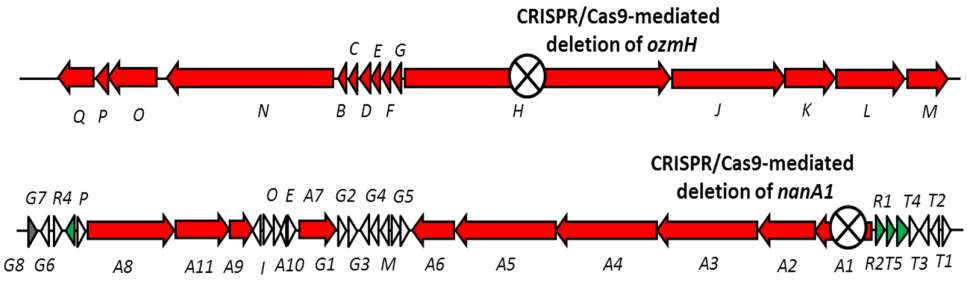

Figure S1. Schematic illustration of the disruption of oxazolomycin and nanchangmycin BGCs via CRISPR/Cas9 mediated genetic manipulation.

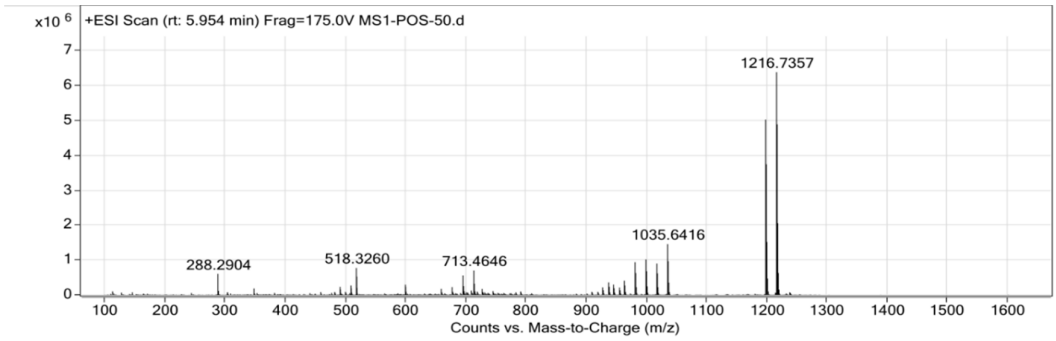

Figure S2. High resolution mass spectrum of meijiemycin.

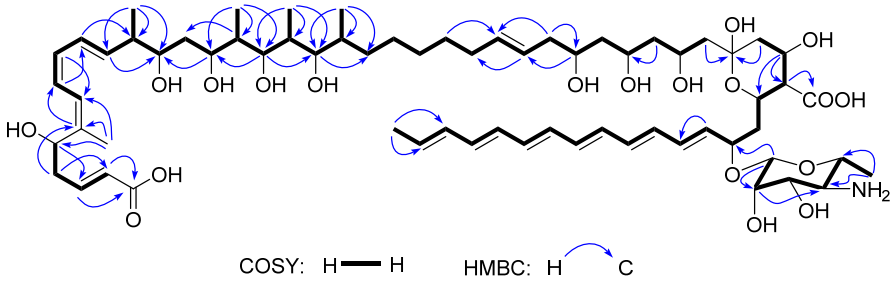

Figure S3. Observed COSY and key HMBC correlations of meijiemycin.

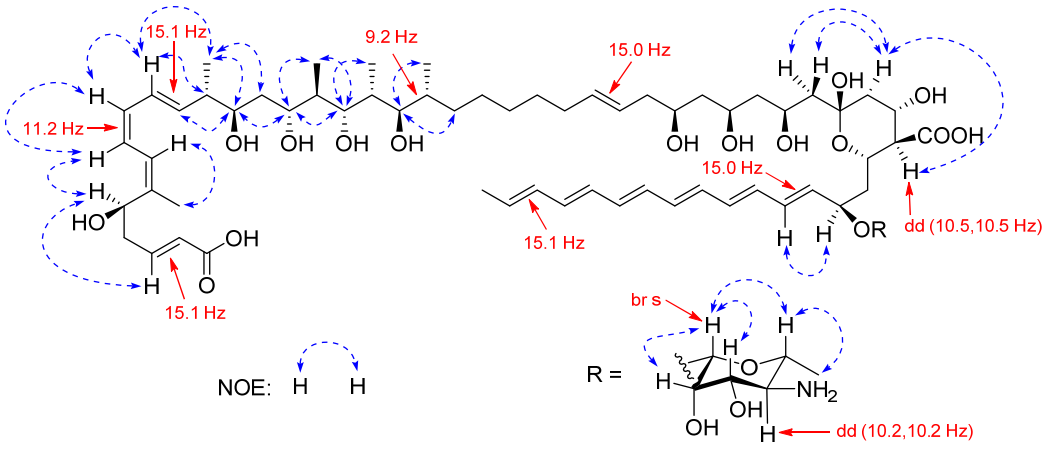

Figure S4. Diagnostic ^{1}H-^{1}H coupling constants (red) and NOE correlations (blue arrows) of meijiemycin.

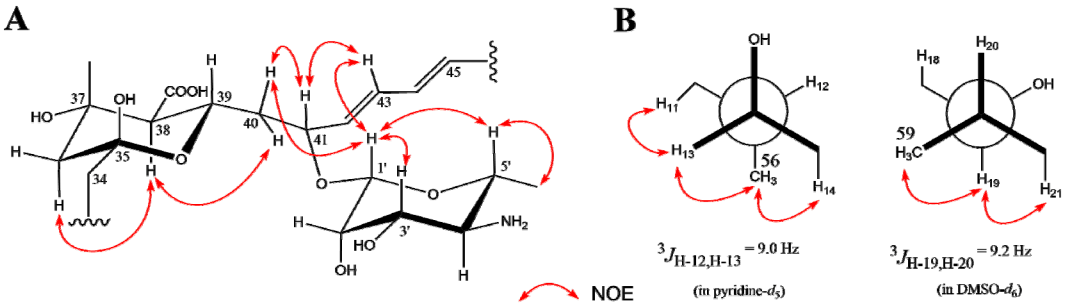

Figure S5. Relative configuration assignment of the hemiketal ring (A), C-12/C-13 and C-19/C-20 (B) in meijiemycin (**1**) based on the coupling constants and NOE correlations.

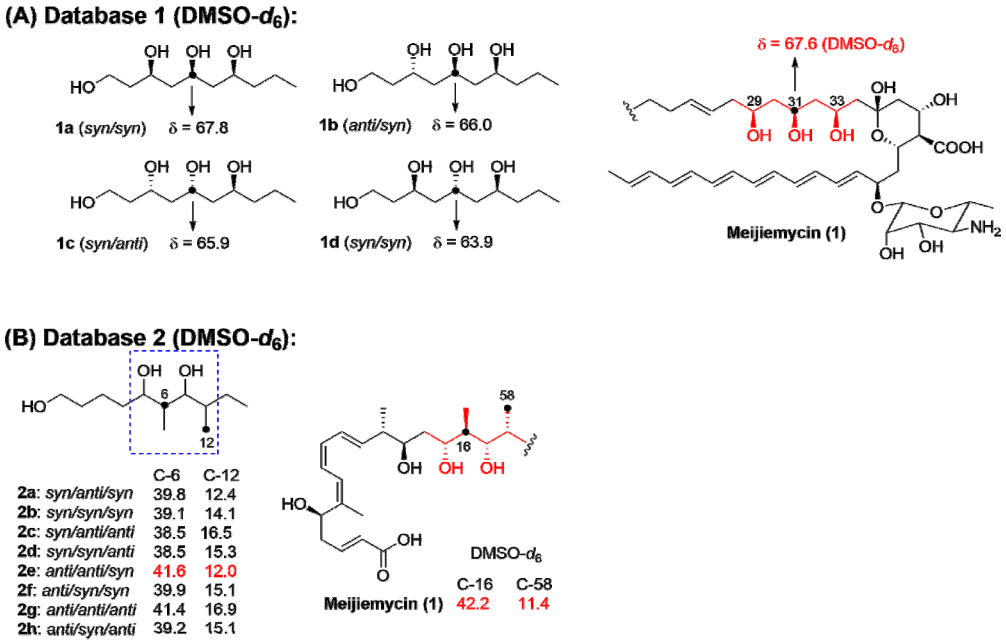

Figure S6. Relative configuration assignment of meijiemycin (**1**) based on the Kishi's universal NMR databases.[20,21] (A) Kishi's NMR database 1 for elucidation of the relative configuration of C-29/C-31/C-33 of meijiemycin. The database 1 showed that the ^{13}C chemical shifts for the central carbons of the triols are classified into three subgroups, with *syn/syn* clustering round δ 68, *syn/anti* and *anti/syn* round δ 66, and *anti/anti* around δ 64. Comparison of the NMR data with the chemical shift (C-31: δ 67.6) of the correponding triol unit in mejiemycin could establish the relative configuration of C-29/C-31/C-33 as *syn/syn*. (B) Kishi's NMR database 2 for elucidation of the relative configuration of C-15/C-16/C-17/C-18 of meijiemycin. The chemical shifts of C-16 and C-58 in meijiemycin were in good agreement with the *anti/anti/syn* mode (**2e**), indicating C-15/C-16/C-17/C-18 possess the same *anti/anti/syn* configuration.

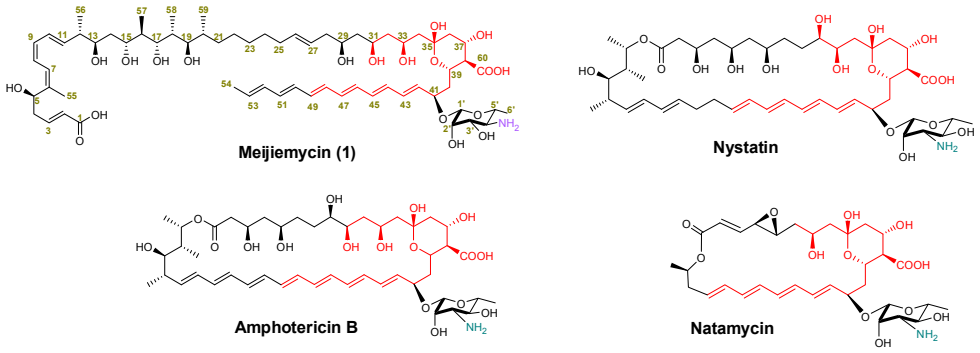

Figure S7. Structures of meijiemycin and the three antifungal macrocyclic polyene-polyols currently used as antifungal drugs. The structural backbone shared by the four compounds is highlighted in red.

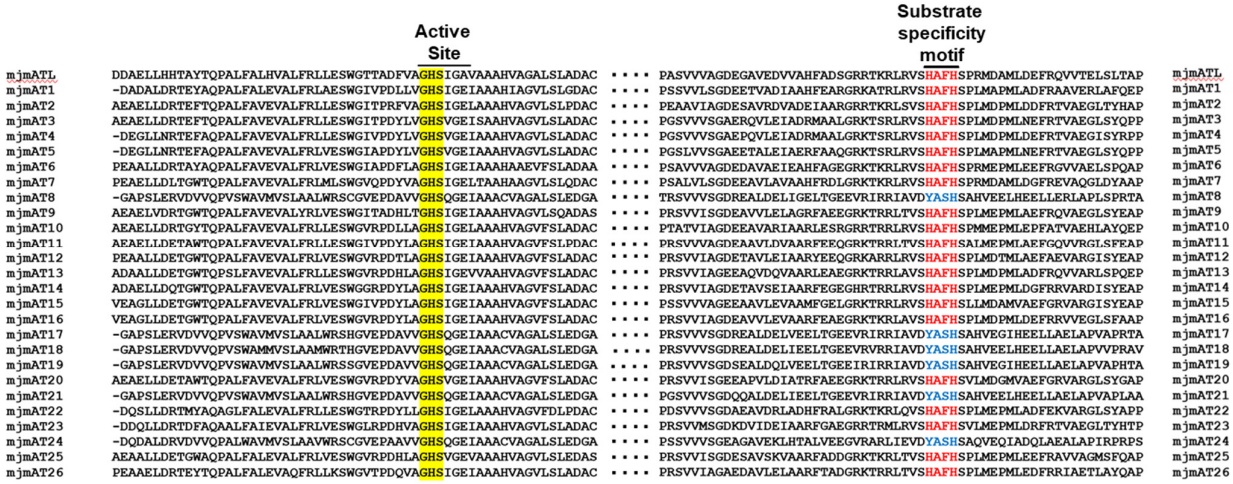

Figure S8. Partial sequence comparison for the AT domains of Mjm PKS modules. Analysis of AT domains show that all of them possess a GHSXG motif[25] at the active site. Malonyl-CoA specificity is determined by HAFH motif in red font while YASH motif in blue font selects for methylmalonyl CoA as substrate.[26]

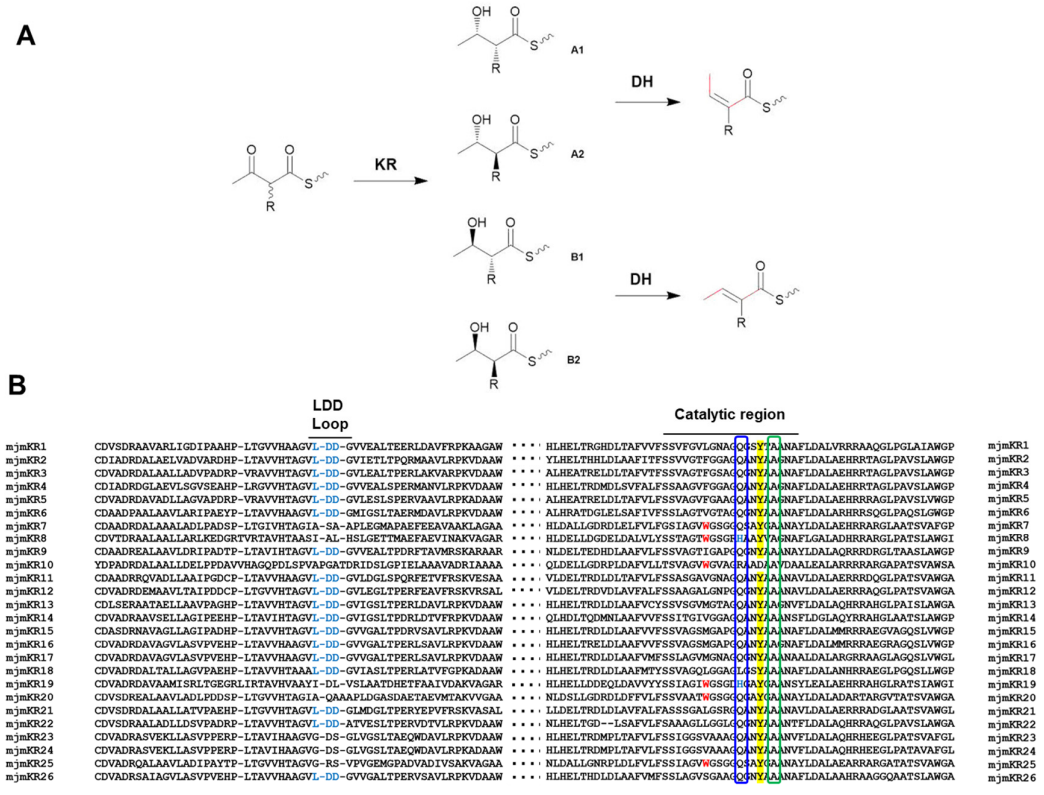

Figure S9. Partial sequence comparison for the KR domains of Mjm PKS modules**.** (A) The KR domains exert stereo control over the geometry of hydroxyl and succeeding olefin moieties. A-type KR reduces β-keto group into a S-hydroxyl group that is subsequently dehydrated into a *cis*-olefin moiety, while B-type KR reduces β-keto group into a R-hydroxyl group that is subsequently dehydrated into a *trans*-olefin moiety. A2-type KR is differentiated from A1-type KR by presence of histidine residue in the catalytic region (depicted by dark blue column), while B2-type KR is differentiated from B1-type KR by presence of proline in the catalytic region (depicted by green column). (B) The KR domains of Mjm PKS which possesses a tryptophan residue (in red) in their catalytic region were annotated as Type A-type KRs, while those that possesses a LDD loop were annotated as B-type KRs.[27] MjmKR23 and MjmKR24, which contain a GDS motif in place of a LDD loop and lack a tryptophan residue (highlighted in yellow) in their catalytic regions, were determined to be A-type KRs through NMR spectral analysis of meijiemycin.

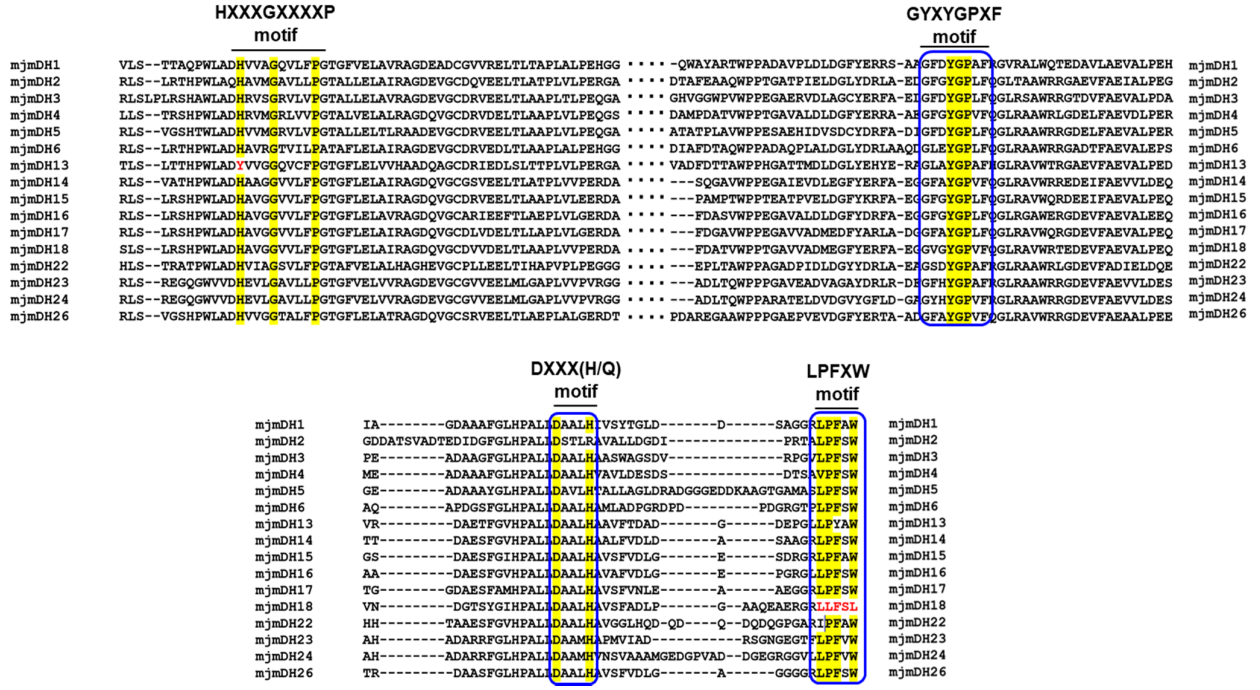

Figure S10. Partial sequence comparison for the DH domains of Mjm PKS modules. All Mjm DH domains possess the crucial HXXXGXXXXP motif involved in the catalytic site,[28] except for MjmDH13, which is likely to be non-functional due to the absence of a histidine residue. Analysis of the LPFXW motif also revealed a missing tryptophan residue for MjmDH18, which is likely the reason for its inactivity.

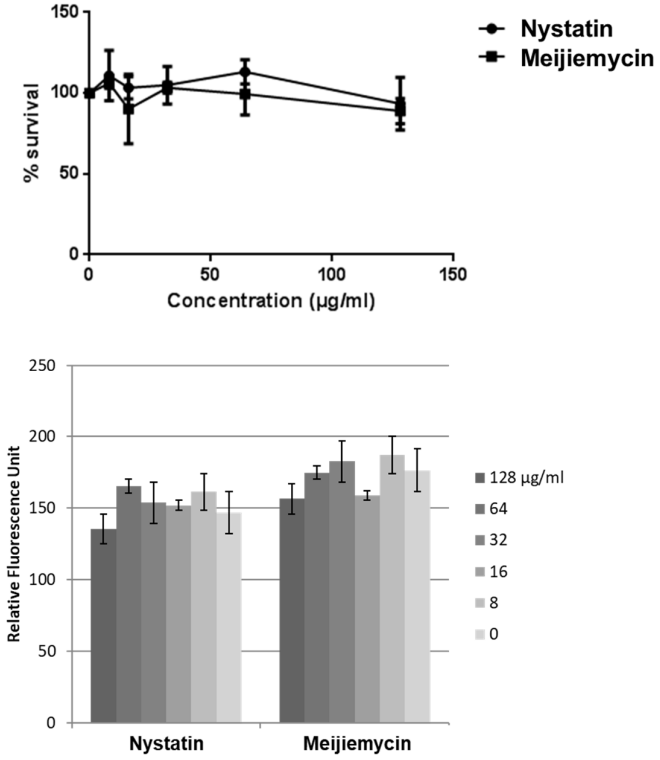

Figure S11. Cytotoxicity assays using the murine RAW264.7 macrophage cell line showed minimal toxicity of meijiemycin up to 128 µg/mL.

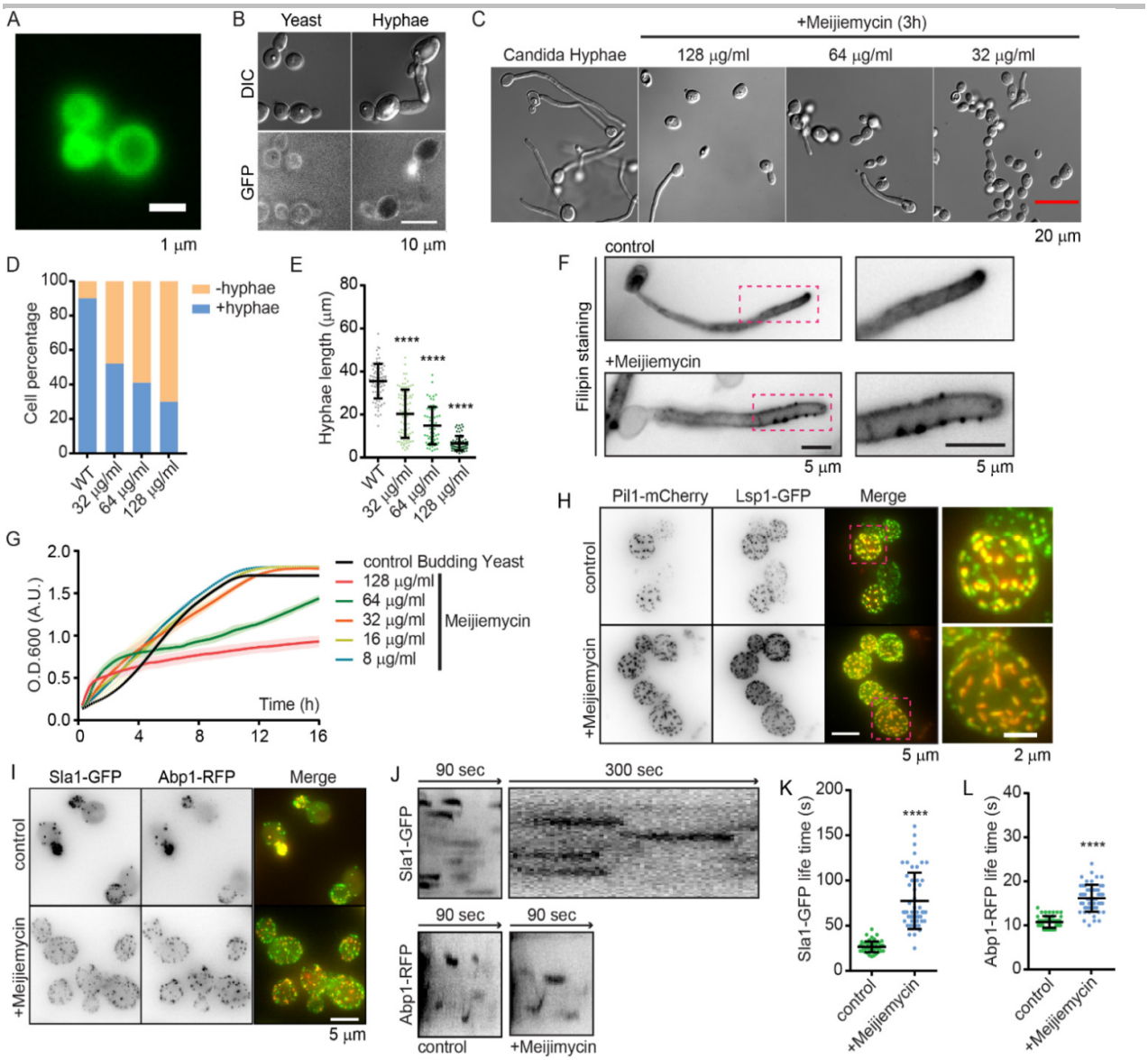

Figure S12. Meijiemycin affects sterol distribution on the plasma membrane and inhibits endocytosis. (A) Glycerophospholipid liposome encapsulation of Alexa Fluor™ 488 labelled meijiemycin. (B) Representative images of *C. albicans* cells treated by liposome encapsulated meijiemycin conjugated with Alexa Fluor™ 488 for 3 hours. (C) Representative differential interference contrast (DIC) images of hyphae cells treated by the indicated dose of meijiemycin for 3 hours in *C. albicans*. (D) Percentage of different doses of meijiemycin treatment on *C. albicans* with or without hyphae formation. (Control, n=144 cells; 32 μg/ml meijiemycin, n=195 cells; 64 μg/ml meijiemycin, n=169 cells; 128 μg/ml meijiemycin, n=262 cells) (E) Quantification of hyphae length of *C. albicans* cells treated by meijiemycin. (Control, n=83 cells; 32 μg/ml meijiemycin, n=83 cells; 64 μg/ml meijiemycin, n=61 cells; 128 μg/ml meijiemycin, n=72 cells) (F) Representative images of *C. albicans* hyphae cells stained by filipin dye, where cells were firstly treated with or without 64 μg/ml meijiemycin for 3 hours. The enlarged regions were indicated by the red box with a dashed line. (G) Liquid growth assay of budding yeast cells treated with meijiemycin compound at the indicated concentration at 30°C. (H) Representative fluorescence images of eisosome marker line (Pil1-mCherry, Lsp1-GFP) treated with or without 32 μg/ml meijiemycin for 3 hours. The enlarged regions were indicated by the red box with the dashed line. (I) Representative fluorescence images of endocytosis marker line (Sla1-GFP, Abp1-RFP) treated with or without 64 μg/ml meijiemycin for 3 hours. (J) Kymograph of Sla1-GFP, Abp1-mRFP lifetime from movies with the indicated time window, where cells were treated with or without 64 μg/ml meijiemycin for 3 hours. (K) Quantification of Sla1-GFP lifetime of the indicated conditions, as in (J). (n=52 endocytic patches for both control and meijiemycin treatment conditions) (L) Quantification of Abp1-RFP lifetime of the indicated conditions, as in (J). (n=54 endocytic patches for control, n=53 endocytic patches for meijiemycin treatment) P-values in (E) was determined by the one-way ANOVA, P-value in (K) and (L) were determined by the two-tailed Student's t-test assuming equal variances, ****p < 0.0001. All the graphs represent mean ± S.D

Figure S13. ^{1}H NMR spectrum (400 MHz, in DMSO-d_6).

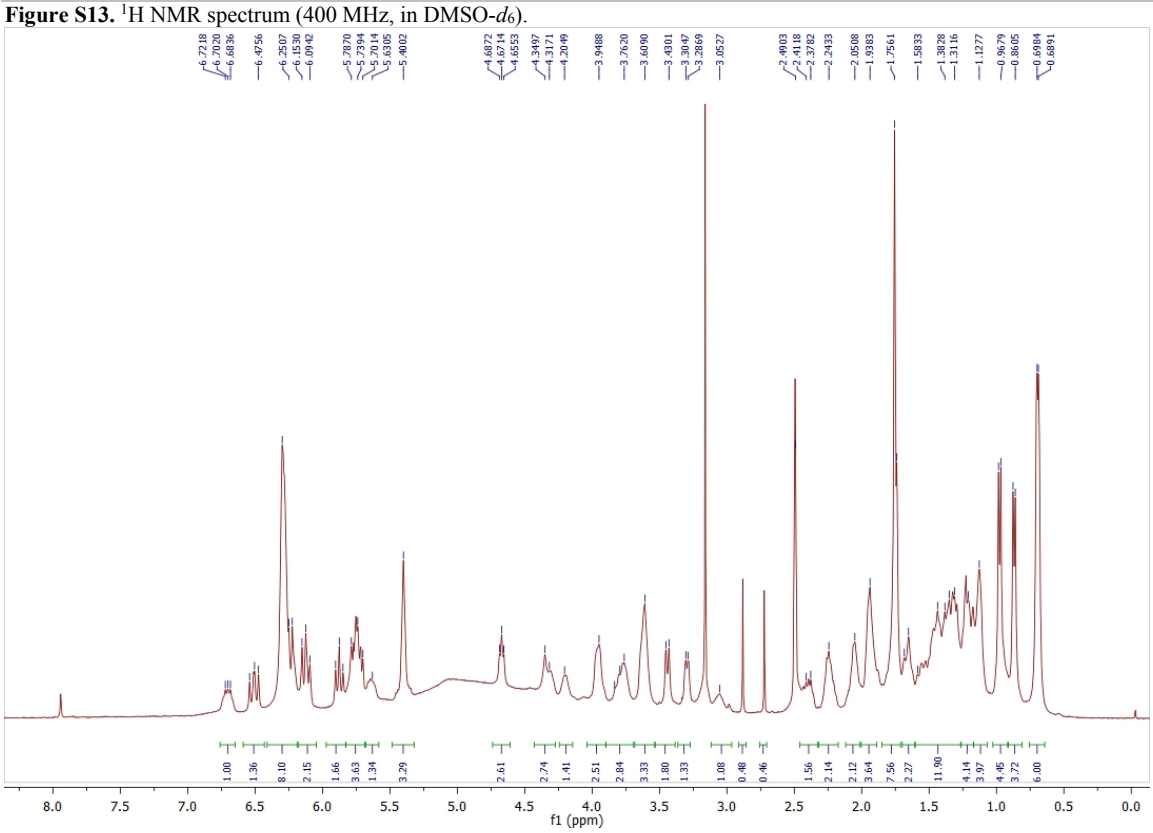

Figure S14. ^{13}C NMR spectrum (400 MHz, in DMSO-d_6).

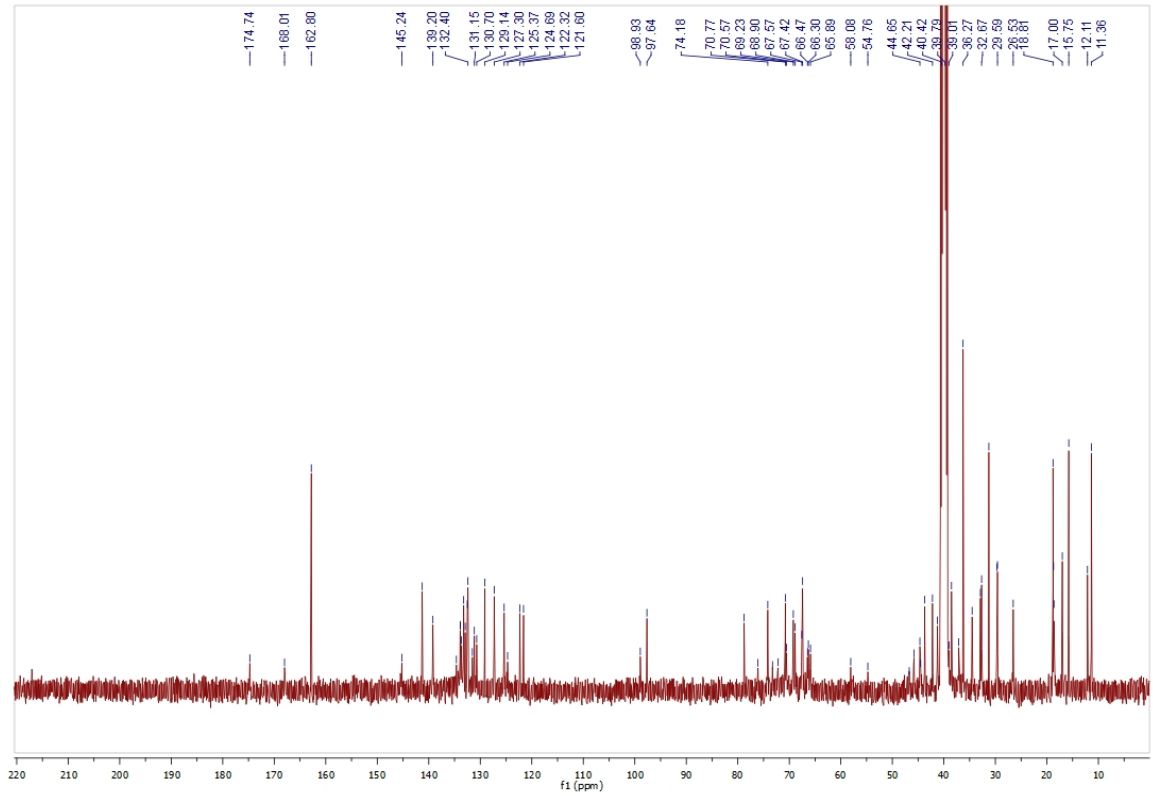

Figure S15. ^{1}H-^{1}H COSY NMR spectrum (400 MHz, in DMSO-d_6).

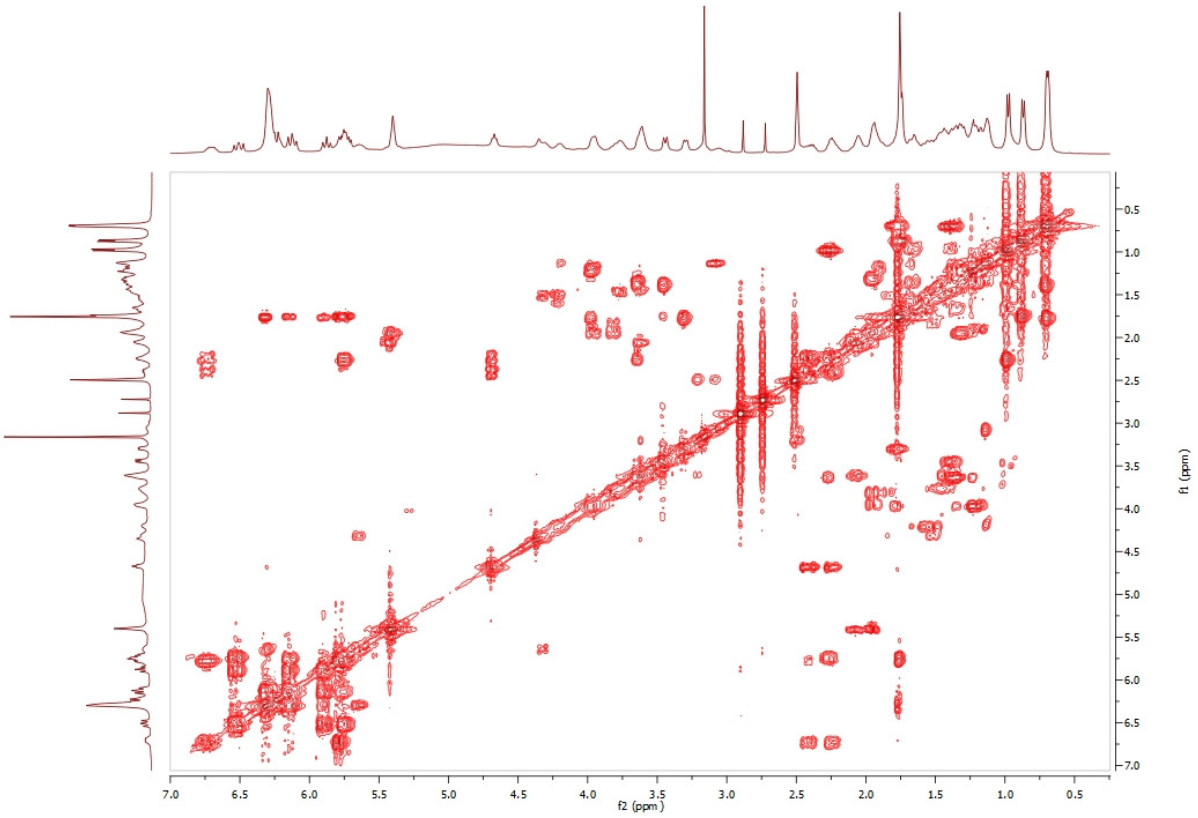

Figure S16. HSQC NMR spectrum (400 MHz, in DMSO-d_6).

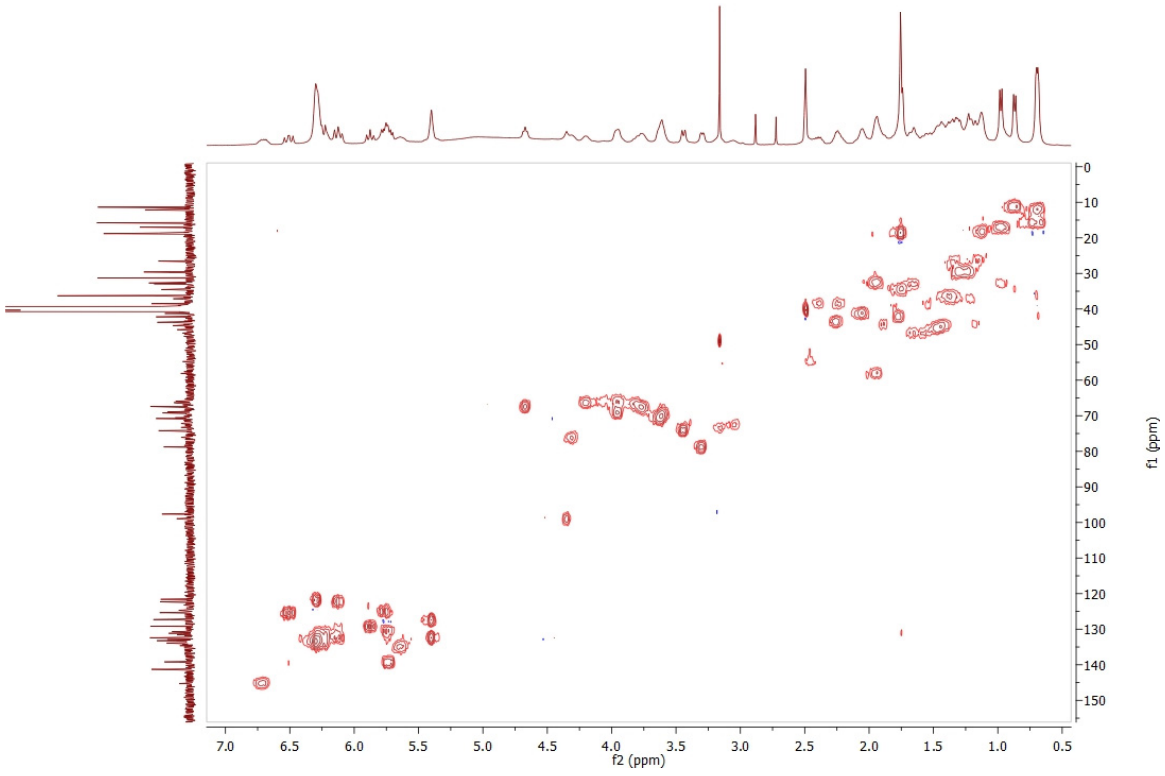

Figure S17. HMBC NMR spectrum (500 MHz, in DMSO-d_6).

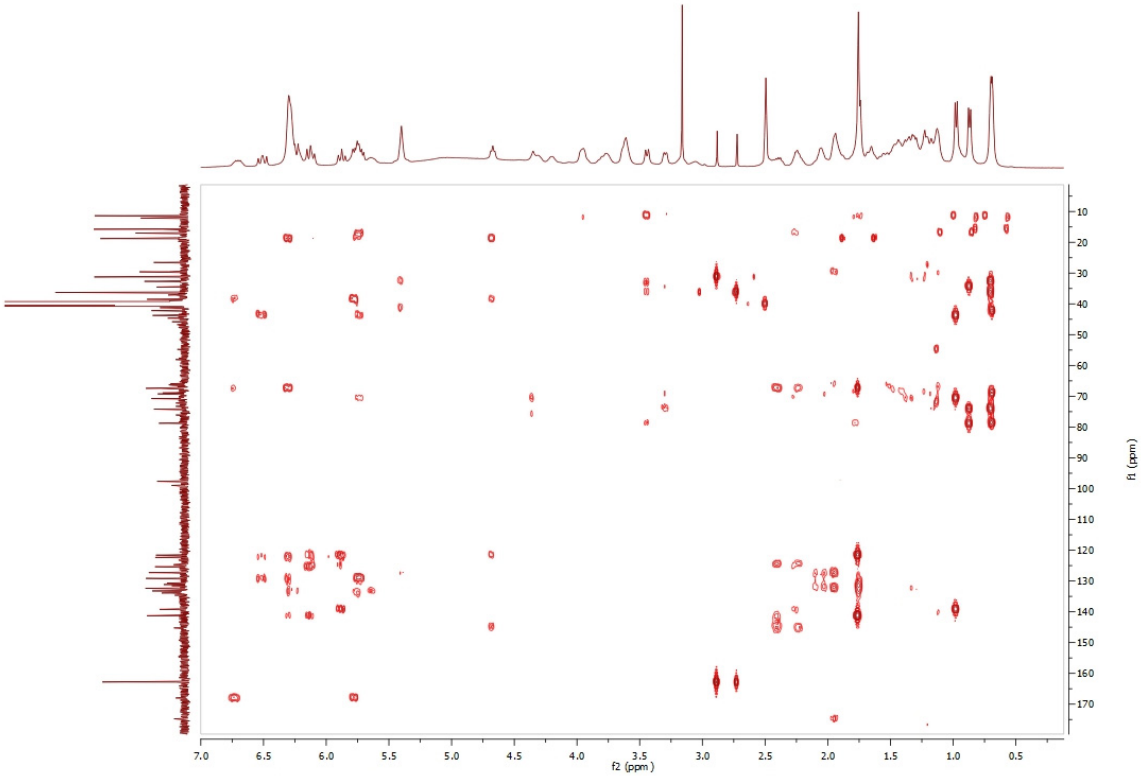

Figure S18. NOESY NMR spectrum (400 MHz, in DMSO-d_6).

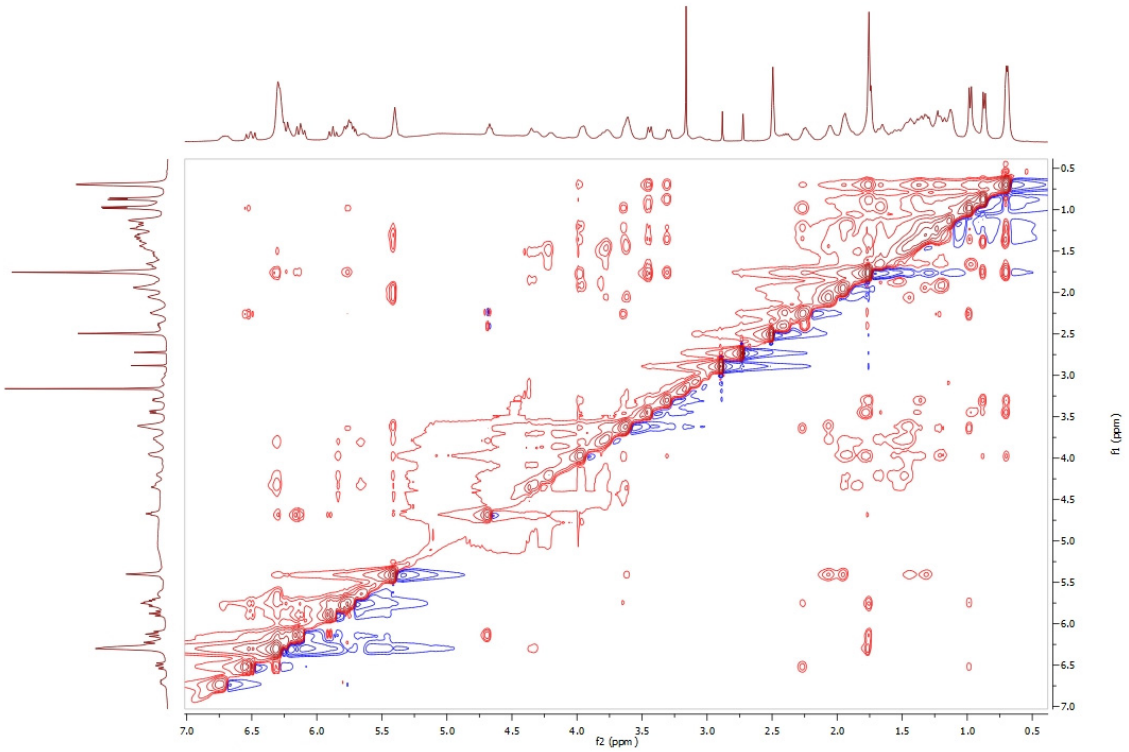

Figure S19. ^{1}H NMR spectrum (400 MHz, in C_5D_5N).

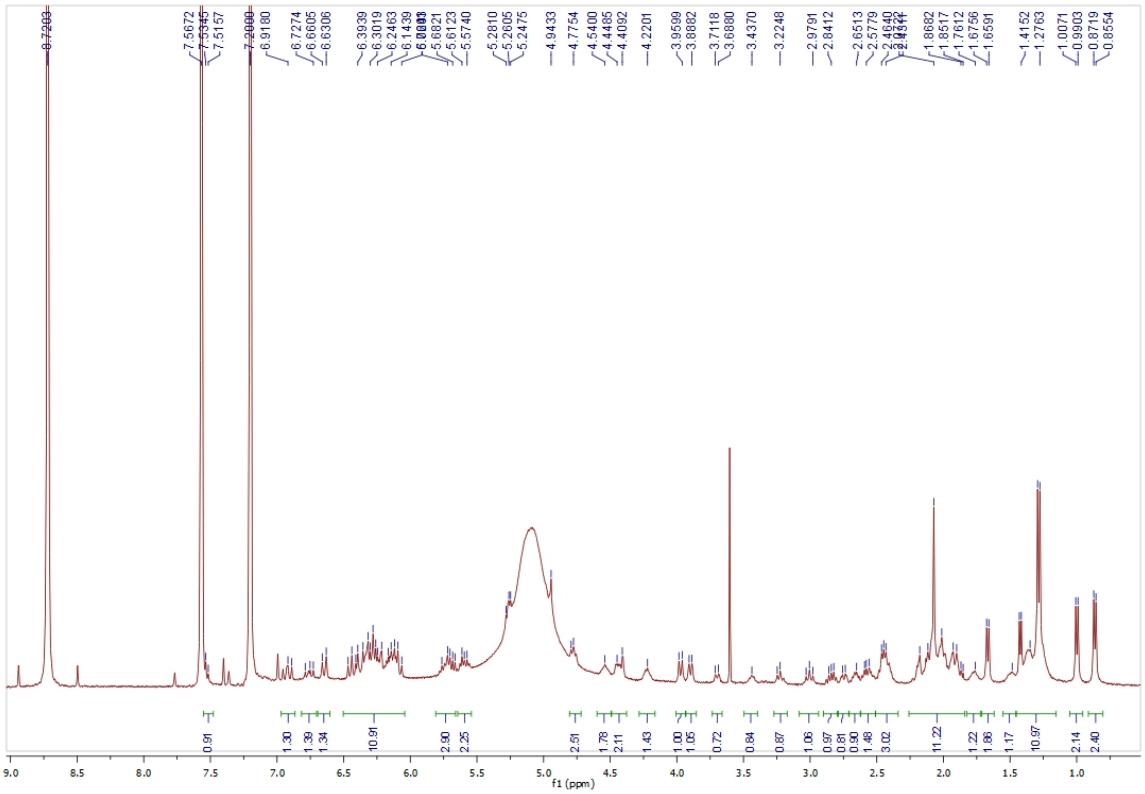

Figure S20. ^{1}H-^{1}H COSY NMR spectrum (400 MHz, in C_5D_5N).

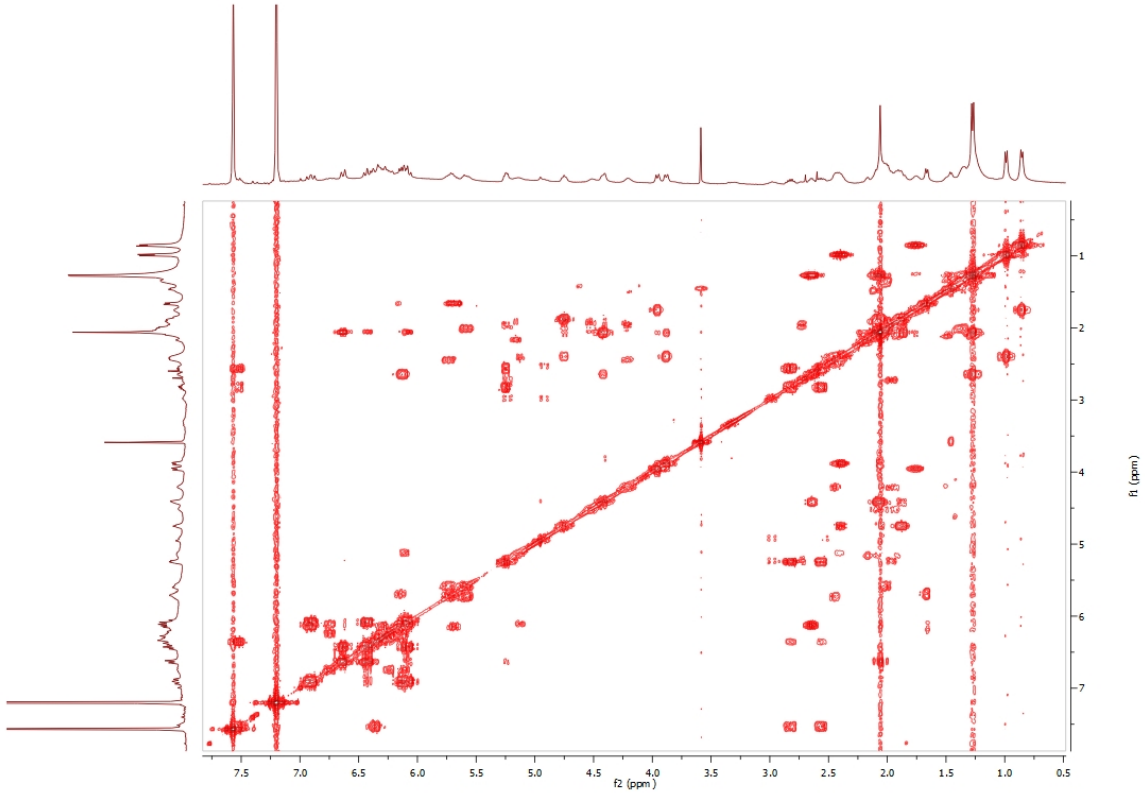

Figure S21. UV spectrum of meijiemycin (**1**).

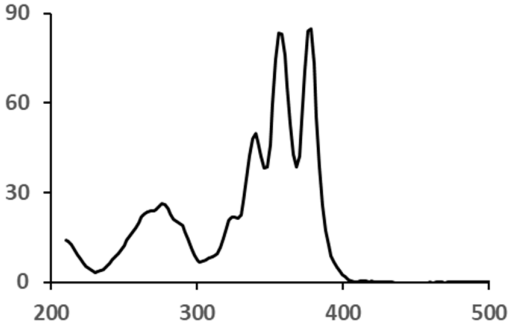

References

1. Pospiech, A.; Neumann, B. *Trends Genet.* **1995**, *11*, 217-218.
2. Koren, S.; Walenz, B. P.; Berlin, K.; Miller, J. R.; Bergman, N. H.; Phillippy, A. M. *Genome Res.* **2017**, *27*, 722-736.
3. Walker, B. J.; Abeel, T.; Shea, T.; Priest, M.; Abouelliel, A.; Sakthikumar, S.; Cuomo, C. A.; Zeng, Q.; Wortman, J.; Young, S. K.; Earl, A. M. *PLoS One* **2014**, *9*, e112963.
4. Low, Z. J.; Pang, L. M.; Ding, Y.; Cheang, Q. W.; Hoang, K.; Tran, H. T.; Li, J.; Liu, X.-W.; Kanagasundaram, Y.; Yang, L.; Liang, Z.-X. *Sci. Rep.* **2018**, *8*, 1594.
5. Liu, D.; Coloe, S.; Baird, R.; Pedersen, J. *J. Clini. Microbiol.* **2000**, *38*, 471-471.
6. Szczeblewski, P.; Laskowski, T.; Bałka, A.; Borowski, E.; Milewski, S. *J. Nat.l Prod.* **2018**, *81*, 1540-1545.
7. Hammond, S. M., Biological activity of polyene antibiotics. In *Progress in Medicinal Chemistry*, Ellis, G. P.; West, G. B. Elsevier: 1977; Vol. 14, pp 105-179.
8. Oroshnik, W; Mebane, A. D. The polyene antifungal antibiotics. *Fortschr. Chem. Org. Naturst* .**1963**, *21*, 17-79.
9. Chen, X.; Guo, Z.; Lai, P. M.; Sze, K. H.; Guo, Z. *Angew. Chem. Int. Ed.* **2010**, *49*, 7926-7928.
10. Gunstone, F. D.; Pollard, M. R.; Scrimgeour, C. M.; Vedanayagam, H. S. *Chem. Physics Lip.* **1977,** *18*, 115-129.
11. Schulze, C. J.; Donia, M. S.; Siqueira-Neto, J. L.; Ray, D.; Raskatov, J. A.; Green, R. E.; McKerrow, J. H.; Fischbach, M. A.; Linington, R. G. *ACS Chem. Biol.* **2015**, *10*, 2373-2381.
12. Udwary, D. W.; Zeigler, L.; Asolkar, R. N.; Singan, V.; Lapidus, A.; Fenical, W.; Jensen, P. R.; Moore, B. S. *Proc. Natl. Acad. Sci. USA* **2007**, *104*, 10376-10381.
13. Szwarc, K.; Szczeblewski, P.; Sowiński, P.; Borowski, E.; Pawlak, J. *J. Antibiot.***2015,** *68*, 504-510.
14. Pawlak, J; Sowiński, P; Borowski, E; Gariboldi, P. *J. Antibiot.* **1993**, *46*, 1598-1604.
15. Sowiński, P; Gariboldi, P; Czerwiński, A; Borowski, E. *J. Antibiot.* **1989**, *42*, 1631-1638.
16. Aparicio, J. F.; Colina, A. J.; Ceballos E.; Martin, J. F. *J. Biol. Chem.* **1999**, *274*, 10133-10139.
17. Caffrey, P.; Lynch, S.; Flood, E.; Finnan S.; Oliynyk, M. *Chem. Biol.* **2001**, *8*, 713-723.
18. Brautaset, T.; Sekurova, O. N.; Sletta, H.; Ellingsen, T. E.; StrLm, A. R.; Valla S.; Zotchev, S. B. *Chem. Biol.* **2000**, *7*, 395-403.
19. Hu, Y.; Wang, M.; Wu, C.; Tan, Y.; Li, J.; Hao, X.; Duan, Y.; Guan, Y.; Shang, X.; Wang, Y.; Xiao, C.; Gan, M. *J. Nat. Prod.* **2017,** *81*, 178-187.
20. Kobayashi, Y.; Tan, C.; Kishi, Y. *J. Am. Chem. Soc.* **2001,** *123*, 2076-2078.
21. Tan, C.; Kobayashi, Y.; Kishi, Y. *Angew. Chem., Int. Ed.* **2000,** 39, 4282-4284.
22. Wiegand, I.; Hilpert, K.; Hancock, R. E.; *Nat. Protoc.* **2008**, *3*, 163-175.
23. Lambert, R. J.; Pearson, J. *J. Appl. Microbiol.* **2000**, *88*, 784-790.
24. Wang, H.; Huang, Z. X.; Au Yong, J. Y.; Zou, H.; Zeng, G.; Gao, J.; Wang, Y.; Wong, A. H. H.; Wang, Y. *Molecular microbiol.* **2016**, *101*, 250-264.
25. Haydock, S. F.; Aparicio, J. F.; Molnár, I.; Schwecke, T.; Khaw, L. E.; König, A.; Marsden, A. F. A.; Galloway, I. S.; Staunton, J.; Leadlay, P. F. *FEBS Lett.* **1995**, *374*, 246-248.
26. Del Vecchio, F. Petkovic, H.; Kendrew, S. G.; Low, L.; Wilkinson, B.; Lill, R.; Cortes, J.; Rudd, B. A.; Staunton, J.; Leadlay, P. F. *J. Ind. Microbiol. Biotechnol.* **2003**, *30*, 489-494.
27. Keatinge-Clay, A. T. *Chem Biol* **2007**, *14*, 898-908.
28. Keatinge-Clay, A. *J Mol Biol* **2008**, *384*, 941-953.

Author Contributions

ZJL and LMP isolated the SD50 strain and sequenced the whole genome. ZJL, JX, GLM and JFH isolated meijiemycin and determined its structure. GLM and PL prepared dye-conjugated meijiemycin. ZJL preformed antifungal assays and performed gene knockout with the assistance of HTT. YX and YM performed the mechanistic studies with C. albicans and budding yeast. HS and WSL optimized the fermentation for meijiemycin production. JF and LY preformed cytotoxicity assays. ZJL, JX, YX, YM and ZXL wrote the manuscript with input from other co-authors.